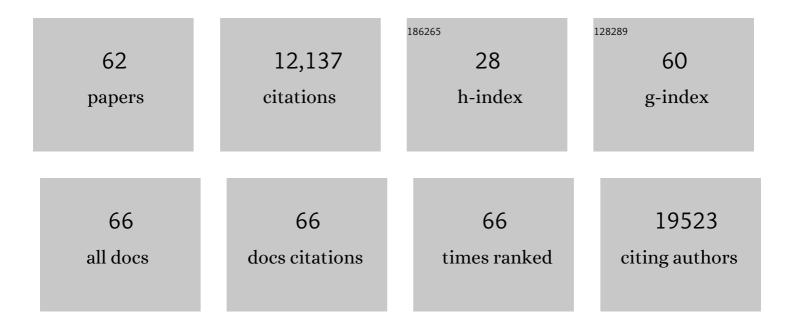
Hisato Yamaguchi

List of Publications by Year in descending order

Source: https://exaly.com/author-pdf/5603990/publications.pdf Version: 2024-02-01



#	Article	IF	CITATIONS
1	Photoluminescence from Chemically Exfoliated MoS ₂ . Nano Letters, 2011, 11, 5111-5116.	9.1	3,402
2	Enhanced catalytic activity in strained chemically exfoliated WS2 nanosheets for hydrogen evolution. Nature Materials, 2013, 12, 850-855.	27.5	2,326
3	Blue Photoluminescence from Chemically Derived Graphene Oxide. Advanced Materials, 2010, 22, 505-509.	21.0	1,824
4	Coherent Atomic and Electronic Heterostructures of Single-Layer MoS ₂ . ACS Nano, 2012, 6, 7311-7317.	14.6	806
5	Tunable Photoluminescence from Graphene Oxide. Angewandte Chemie - International Edition, 2012, 51, 6662-6666.	13.8	584
6	Insulator to Semimetal Transition in Graphene Oxide. Journal of Physical Chemistry C, 2009, 113, 15768-15771.	3.1	577
7	Evolution of the Electronic Band Structure and Efficient Photo-Detection in Atomic Layers of InSe. ACS Nano, 2014, 8, 1263-1272.	14.6	534
8	Graphene and Mobile Ions: The Key to All-Plastic, Solution-Processed Light-Emitting Devices. ACS Nano, 2010, 4, 637-642.	14.6	266
9	Highly Uniform 300 mm Wafer-Scale Deposition of Single and Multilayered Chemically Derived Graphene Thin Films. ACS Nano, 2010, 4, 524-528.	14.6	209
10	Chemically exfoliated ReS ₂ nanosheets. Nanoscale, 2014, 6, 12458-12462.	5.6	160
11	Field Emission from Atomically Thin Edges of Reduced Graphene Oxide. ACS Nano, 2011, 5, 4945-4952.	14.6	139
12	Electronic Structure and Chemical Nature of Oxygen Dopant States in Carbon Nanotubes. ACS Nano, 2014, 8, 10782-10789.	14.6	131
13	Flexible and Metal-Free Light-Emitting Electrochemical Cells Based on Graphene and PEDOT-PSS as the Electrode Materials. ACS Nano, 2011, 5, 574-580.	14.6	110
14	Graphene Supported MoS ₂ Structures with High Defect Density for an Efficient HER Electrocatalysts. ACS Applied Materials & Interfaces, 2020, 12, 12629-12638.	8.0	101
15	Flame synthesis of graphene films in open environments. Carbon, 2011, 49, 5064-5070.	10.3	90
16	Tuning the Fröhlich exciton-phonon scattering in monolayer MoS2. Nature Communications, 2019, 10, 807.	12.8	65
17	Reduced Graphene Oxide Thin Films as Ultrabarriers for Organic Electronics. Advanced Energy Materials, 2014, 4, 1300986.	19.5	59
18	Free-standing graphene on microstructured silicon vertices for enhanced field emission properties. Nanoscale, 2012, 4, 3069.	5.6	58

HISATO YAMAGUCHI

#	Article	IF	CITATIONS
19	Spatially Resolved Photoexcited Charge-Carrier Dynamics in Phase-Engineered Monolayer MoS ₂ . ACS Nano, 2015, 9, 840-849.	14.6	58
20	Opto-valleytronic imaging of atomically thin semiconductors. Nature Nanotechnology, 2017, 12, 329-334.	31.5	55
21	Development of an Amorphous Selenium-Based Photodetector Driven by a Diamond Cold Cathode. Sensors, 2013, 13, 13744-13778.	3.8	41
22	Field emission from reconstructed heavily phosphorus-doped homoepitaxial diamond (111). Applied Physics Letters, 2006, 88, 212114.	3.3	39
23	Perspectives on Designer Photocathodes for X-ray Free-Electron Lasers: Influencing Emission Properties with Heterostructures and Nanoengineered Electronic States. Physical Review Applied, 2018, 10, .	3.8	36
24	Ultrafast Optical Microscopy of Single Monolayer Molybdenum Disulfide Flakes. Scientific Reports, 2016, 6, 21601.	3.3	35
25	xmins:mml="http://www.w3.org/1998/Wath/Wath/WL"> <mml:mrow><mml:mi>Wo</mml:mi><mml:msub><mml:m mathvariant="normal">S<mml:mn>2</mml:mn></mml:m </mml:msub></mml:mrow> on <mml:math xmlns:mml="http://www.w3.org/1998/Math/MathML"><mml:mrow><mml:mi>Si</mml:mi>Sito the term of term of</mml:mrow></mml:math 	ii 3.2	35
26	Direct Imaging of Charge Transport in Progressively Reduced Graphene Oxide Using Electrostatic Force Microscopy. ACS Nano, 2015, 9, 2981-2988.	14.6	29
27	Field emission mechanism of oxidized highly phosphorus-doped homoepitaxial diamond (111). Applied Physics Letters, 2005, 87, 234107.	3.3	24
28	Active bialkali photocathodes on free-standing graphene substrates. Npj 2D Materials and Applications, 2017, 1, .	7.9	24
29	Electron emission mechanism of diamond characterized using combined x-ray photoelectron spectroscopy/ultraviolet photoelectron spectroscopy/field emission spectroscopy system. Applied Physics Letters, 2006, 88, 202101.	3.3	21
30	Field emission from surfaceâ€modified heavily phosphorusâ€doped homoepitaxial (111) diamond. Physica Status Solidi (A) Applications and Materials Science, 2007, 204, 2957-2964.	1.8	21
31	A photoemission moments model using density functional and transfer matrix methods applied to coating layers on surfaces: Theory. Journal of Applied Physics, 2018, 123, .	2.5	15
32	Free‣tanding Bialkali Photocathodes Using Atomically Thin Substrates. Advanced Materials Interfaces, 2018, 5, 1800249.	3.7	14
33	Broad area electron emission from oxygen absorbed homoepitaxially grown nitrogen (N)-doped chemical vapor deposited diamond (111) surface. Journal of Vacuum Science & Technology an Official Journal of the American Vacuum Society B, Microelectronics Processing and Phenomena, 2003, 21, 1730.	1.6	13
34	Valenceâ€band electronic structure evolution of graphene oxide upon thermal annealing for optoelectronics. Physica Status Solidi (A) Applications and Materials Science, 2016, 213, 2380-2386.	1.8	13
35	Opto-electro-mechanical percolative composites from 2D layered materials: Properties and applications in strain sensing. Composites Science and Technology, 2019, 182, 107687.	7.8	13
36	Diode structure amorphous selenium photodetector with nitrogen (N)-doped diamond cold cathode. Journal of Vacuum Science & Technology an Official Journal of the American Vacuum Society B, Microelectronics Processing and Phenomena, 2003, 21, 1586.	1.6	10

HISATO YAMAGUCHI

#	Article	IF	CITATIONS
37	Field Emission from Modified P-Doped Diamond Surfaces with Different Barrier Heights. Japanese Journal of Applied Physics, 2008, 47, 8921-8924.	1.5	10
38	Effects of Synthesis Parameters on CVD Molybdenum Disulfide Growth. MRS Advances, 2016, 1, 2291-2296.	0.9	9
39	Field emission process of O-terminated heavily P-doped homoepitaxial diamond. Diamond and Related Materials, 2006, 15, 863-865.	3.9	8
40	Field emission characteristics of surface-reconstructed heavily phosphorus-doped homoepitaxial diamond. Journal of Vacuum Science & Technology B, 2007, 25, 528.	1.3	8
41	Nonlinear Absorption and Photocurrent in Weyl Semimetals. Physica Status Solidi (B): Basic Research, 2019, 256, 1900305.	1.5	8
42	Photoemission from Bialkali Photocathodes through an Atomically Thin Protection Layer. ACS Applied Materials & Interfaces, 2022, 14, 1710-1717.	8.0	8
43	Amorphous selenium based photodetector driven by field emission current from N-doped diamond cold cathode. Journal of Vacuum Science & Technology B, 2006, 24, 1035.	1.3	7
44	Polariton hyperspectral imaging of two-dimensional semiconductor crystals. Scientific Reports, 2019, 9, 13756.	3.3	7
45	Characterization of 2D MoS2 and WS2 Dispersed in Organic Solvents for Composite Applications. MRS Advances, 2016, 1, 2303-2308.	0.9	6
46	Quantum Efficiency Enhancement of Bialkali Photocathodes by an Atomically Thin Layer on Substrates. Physica Status Solidi (A) Applications and Materials Science, 2019, 216, 1900501.	1.8	6
47	An extended moments model of quantum efficiency for metals and semiconductors. Journal of Applied Physics, 2020, 128, .	2.5	6
48	Gas Barrier Properties of Chemical Vapor-Deposited Graphene to Oxygen Imparted with Sub-electronvolt Kinetic Energy. Journal of Physical Chemistry Letters, 2020, 11, 9159-9164.	4.6	5
49	Graphene as reusable substrate for bialkali photocathodes. Applied Physics Letters, 2020, 116, 251903.	3.3	5
50	Signatures of defect-localized charged excitons in the photoluminescence of monolayer molybdenum disulfide. Physical Review Materials, 2018, 2, .	2.4	5
51	Sensitivity to red/green/blue illumination of amorphous selenium based photodetector driven by nitrogen (N)-Doped CVD diamond. Diamond and Related Materials, 2008, 17, 95-99.	3.9	4
52	Clarification of band structure at metal–diamond contact using device simulation. Applied Surface Science, 2008, 254, 6285-6288.	6.1	3
53	Direct Heteroepitaxy of Orientationâ€Patterned GaP on GaAs by Hydride Vapor Phase Epitaxy for Quasiâ€Phaseâ€Matching Applications. Physica Status Solidi (A) Applications and Materials Science, 2020, 217, 1900627.	1.8	3
54	Electron emission from heavily nitrogen-doped heteroepitaxial chemical vapor deposition diamond. Journal of Vacuum Science & Technology an Official Journal of the American Vacuum Society B, Microelectronics Processing and Phenomena, 2004, 22, 1327.	1.6	2

#	Article	IF	CITATIONS
55	Angular scattering of protons through ultrathin graphene foils: Application for time-of-flight instrumentation. Review of Scientific Instruments, 2020, 91, 033302.	1.3	2
56	Direct Heteroepitaxy and Selective Area Growth of GaP and GaAs on Si by Hydride Vapor Phase Epitaxy. Physica Status Solidi (A) Applications and Materials Science, 2021, 218, 2000447.	1.8	2
57	Large area deposition of graphene thin films by Langmuir-Blodgett assembly and their optoelectronic properties. , 2009, , .		1
58	Photocathode: Free-Standing Bialkali Photocathodes Using Atomically Thin Substrates (Adv. Mater.) Tj ETQq0 0 () rgBT /O\ 9.7	rerlock 10 Tf 5
59	The Origin of Field-induced Electron Emission from N-doped CVD Diamond Characterized by Combined XPS/UPS/FES System. Materials Research Society Symposia Proceedings, 2007, 1039, 1.	0.1	0
60	Barrier Height Difference Induced by Surface Terminations for Field Emission from P-doped Diamond. Materials Research Society Symposia Proceedings, 2007, 1039, 1.	0.1	0

61	Field Emission Mechanism of H-Terminated N-Type Diamond NEA Surface. Materials Research Society Symposia Proceedings, 2012, 1395, 51.	0.1	0
62	Development of Orientation-Patterned GaP Growth on GaAs for Nonlinear Frequency Conversion. ,		0

62 2019, , .